

Chemical Science

π -Dimerization of viologen subunits around the core of C₆₀ from twelve to six directions

Julien Iehl,^a Marco Frasconi,^a Henri-Pierre Jacquot de Rouville,^a Nicolas Renaud,^a Scott M. Dyar,^{ab} Nathan L. Strutt,^a Ranaan Carmieli,^{ab} Michael R. Wasielewski,^{ab} Mark A. Ratner,^a Jean-François Nierengarten^c and J. Fraser Stoddart^{a*}

^a Department of Chemistry, Northwestern University, 2145 Sheridan Road, Evanston, IL, 60208-3113, USA. E-mail: stoddart@northwestern.edu

^b Argonne-Northwestern Solar Energy Research (ANSER) Center, Northwestern University, Evanston, Illinois 60208, USA

^c Laboratoire de Chimie des Matériaux Moléculaires Université de Strasbourg et CNRS Ecole Européenne de Chimie, Polymères et Matériaux 25 rue Becquerel, 67087 Strasbourg Cedex 2, France

SUPPORTING INFORMATION

Table of Contents

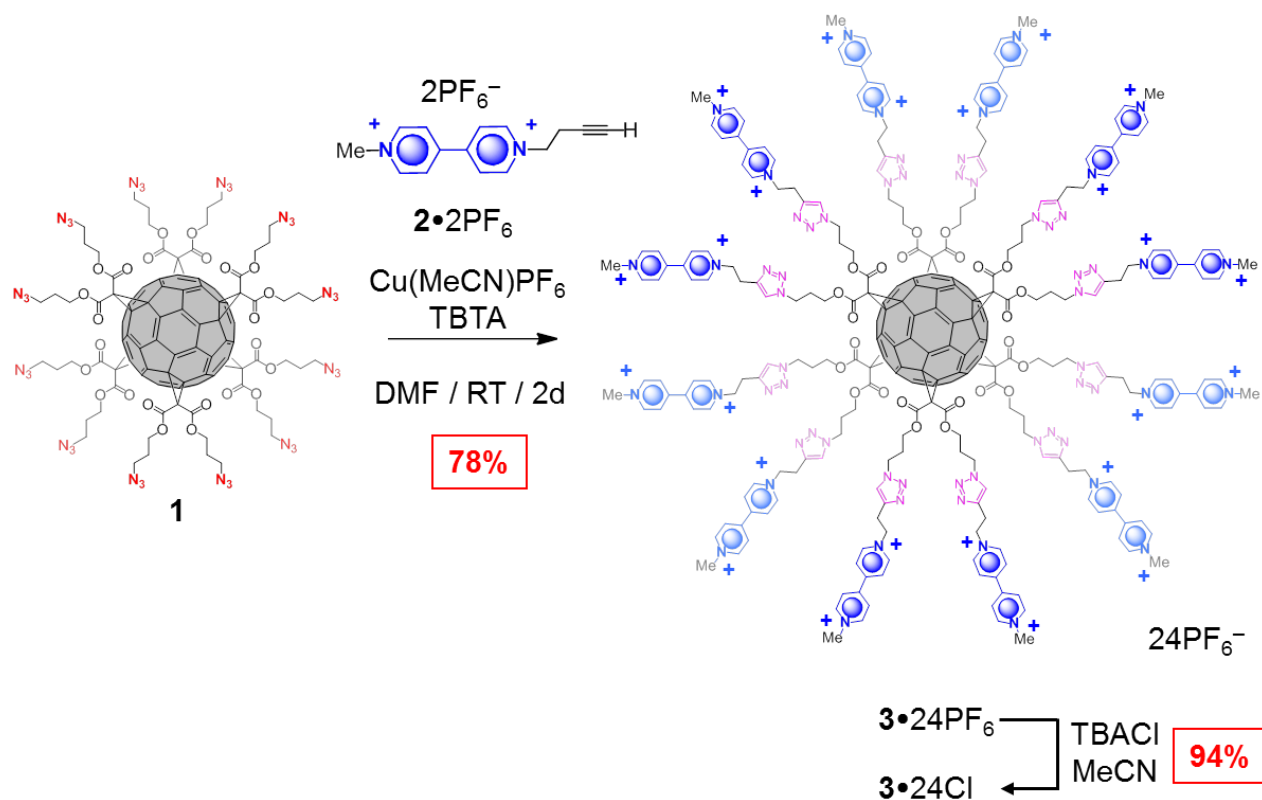
S1.	General methods.....	S2
S2.	Synthetic protocols.....	S3
S3.	¹ H and ¹³ C NMR spectroscopy.....	S6
S4.	Mass spectrometry.....	S14
S5.	Electrochemical experiments.....	S16
S6.	UV/Vis spectroscopy.....	S18
S7.	EPR spectroscopy.....	S20
S8.	Theoretical investigation.....	S20
S9.	Supplementary references.....	S24

S1. General methods

Starting materials and reagents were purchased from Aldrich or Fisher and used as received. Compounds **1**^{S1} and **2**•2PF₆^{S2} were prepared following procedures reported in the literature. All reactions were performed under an atmosphere of nitrogen and in dry solvents, unless otherwise stated. Analytical thin-layer chromatography (TLC) was performed on aluminum sheets, precoated with silica gel 60-F254 (Merck 5554). Flash chromatography was carried out using silica gel 60 (Silicycle) as the stationary phase. UV/Vis spectra were recorded with TU-1800pc UV-Vis spectrophotometer at 273 K unless otherwise stated. Nuclear magnetic resonance (NMR) spectra were recorded at 298 K on a Bruker Avance 500 spectrometer, with a working frequency of 500 MHz for ¹H. Chemical shifts are reported in ppm relative to the signal corresponding to the residual non-deuterated solvent (CD₃CN: δ 1.94 ppm; D₂O; δ 4.79 ppm; MeOD: δ 3.31 ppm). EPR Measurements at X-band (9.5 GHz) were carried out using a Bruker Elexsys E580-X EPR spectrometer outfitted with a variable Q dielectric resonator (ER-4118X-MD5-W1). All the samples were dissolved in degassed appropriate solvent (MeCN, DMF or H₂O) and prepared in a N₂-filled glove box to ensure the absence of oxygen. Samples were loaded into quartz tubes (1.5 mm I.D. x 1.8 mm O.D.) and sealed with a clear ridged UV doming epoxy (Epoxies, Etc., DC-7160 UV). All the samples were used immediately after preparation. Steady-state CW EPR spectra were measured at X-band using 2 mW microwave power and 1 G modulation amplitude at 100 KHz, with a time constant of 2.56 ms and a conversion time of 20.48 ms. Cyclic voltammetry (CV) experiments were carried out at room temperature, unless otherwise stated, in argon-purged solutions in MeCN with a Gamry Multipurpose instrument (Reference 600) interfaced to a PC. CV Experiments were performed using a glassy carbon working electrode (0.071 cm², Cypress system). The electrode surface was polished routinely

with 0.05 μm alumina-water slurry on a felt surface immediately before use. The counter electrode was a Pt coil and the reference electrode was a saturated calomel electrode. Experimental errors: potential values, ± 10 mV. Spectroelectrochemistry (SEC) experiments were carried out using a custom-built optically-transparent thin-layer electrochemical (OTTLE) cell with an optical path of 2 mm, using a Pt grid as working electrode, a Pt wire as counter electrode and a Ag wire pseudo-reference electrode. High resolution electrospray ionization (HR-ESI) mass spectra were measured on Agilent 6210 LC-TOF with Agilent 1200 HPLC introduction.

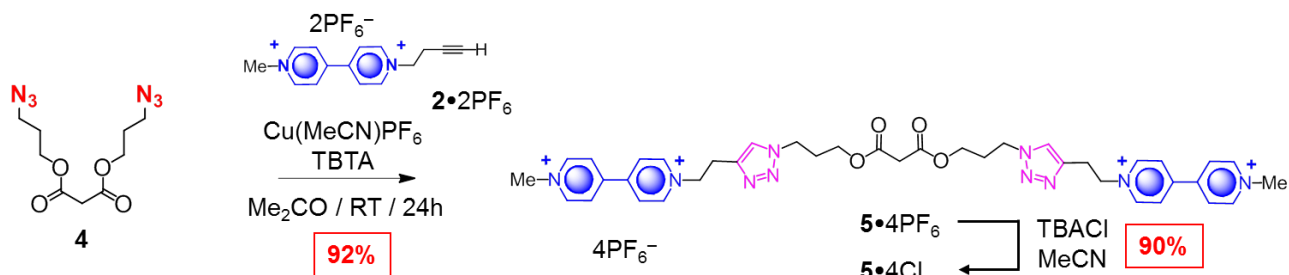
S2. Synthetic protocols



Scheme S1. Synthesis of the hexakis-adducts **3**• 24PF_6 and **3**• 24Cl of C_{60}

3•24PF₆: **1** (50 mg, 0.021 mmol) and **2•2PF₆** (143 mg, 0.278 mmol), tetrakis(acetonitrile) copper(I) hexafluorophosphate (8 mg, 0.018 mmol) and tris[(1-benzyl-1*H*-1,2,3-triazol-4-yl)methyl] amine (TBTA) were dissolved in DMF (2 mL). The reaction mixture was then stirred at room temperature for 2 days. The mixture was subjected to gel permeation chromatography (Biobeads SX-1, DMF) to afford **3•24PF₆** (142 mg, 78%) as an orange glassy product. UV/Vis (MeCN): 284 (sh, 48120), 300 (sh, 40360), 320 (sh, 28480), 336 (sh, 21 960), 390 (sh, 5040); ¹H NMR (500 MHz, CD₃CN, 298 K): δ = 8.90 (d, *J* = 7 Hz, 24H), 8.86 (d, *J* = 7 Hz, 24H), 8.40 (m, 48H), 7.62 (s, 12H), 4.97 (t, *J* = 6 Hz, 24H), 4.41 (s, 36H), 4.37 (t, *J* = 6 Hz, 24H), 4.28 (t, *J* = 6 Hz, 24H), 3.42 (t, *J* = 6 Hz, 24H), 2.20 (m, 24H). ¹³C NMR (125 MHz, CD₃CN, 298 K): δ = 164.3, 151.1, 150.4, 147.4, 146.8, 146.5, 142.7, 142.2, 127.9, 127.7, 124.3, 70.1, 65.3, 62.0, 55.3, 49.6, 47.7, 46.7, 29.7, 27.9. ESI-HRMS: C₂₉₄H₂₆₄F₁₄₄N₆₀O₂₄P₂₄ calcd for *m/z* = 1980.1044 [*M* – 4PF₆]⁴⁺, found *m/z* = 1980.1013; calcd for *m/z* = 1555.0906 [*M* – 5PF₆]⁵⁺, found *m/z* = 1555.0886; calcd for *m/z* = 1271.7480 [*M* – 6PF₆]⁶⁺, found *m/z* = 1271.7435; calcd for *m/z* = 1069.7480 [*M* – 7PF₆]⁷⁺, found *m/z* = 1069.3576.

3•24Cl: **3•24PF₆** (130 mg, 0.015 mmol) was dissolved in a minimum amount of MeCN and saturated aqueous TBACl solution was added dropwise to the resulting solution. The precipitate which was formed was filtered and washed with MeCN to afford **3•24Cl**: (84 mg, 94%) as an orange glassy product. UV/Vis (H₂O): 320 (sh, 42200), 338 (sh, 35920), 384 (sh, 10080); ¹H NMR (500 MHz, D₂O, 298 K): δ = 8.99 (m, 48H), 8.48 (m, 48H), 7.87 (s, 12H), 4.97 (t, *J* = 6 Hz, 24H), 4.45 (s, 36H), 4.37 (t, *J* = 6 Hz, 24H), 4.31 (t, *J* = 6 Hz, 24H), 3.44 (t, *J* = 6 Hz, 24H), 2.20 (m, 24H). ¹³C NMR (125 MHz, D₂O, 298 K): δ = 164.1, 150.4, 149.44, 146.2, 145.4, 145.3, 142.0, 141.0, 127.0, 126.6, 124.1, 69.0, 64.8, 61.0, 48.3, 47.1, 45.7, 28.3, 26.7.



Scheme S2. Synthesis of the reference compounds **5•4PF₆** and **5•4Cl**

5•4PF₆: **4** (50 mg, 0.185 mmol) and **2•2PF₆** (190 mg, 0.37 mmol), tetrakis(acetonitrile) copper(I) hexafluorophosphate (7 mg, 0.018 mmol) and tris[(1-benzyl-1*H*-1,2,3-triazol-4-yl)methyl] amine (TBTA) were dissolved in Me_2CO (3 mL). The mixture was then stirred at room temperature for 24 h before being subjected to column chromatography (SiO_2 , gradient elution from 1% up to 5% NH_4PF_6 in Me_2CO) to afford **5•4PF₆** (220 mg, 92%) as a beige solid. ^1H NMR (500 MHz, CD_3CN , 298 K): δ = 8.84 (d, J = 7 Hz, 8H), 8.36 (m, 8H), 7.64 (s, 2H), 4.96 (t, J = 6 Hz, 4H), 4.39 (m, 10H), 4.02 (t, J = 6 Hz, 4H), 3.43 (t, J = 6 Hz, 4H), 3.36 (s, 12H), 2.17 (m, 4H). ^{13}C NMR (125 MHz, CD_3CN , 298 K): δ = 167.7, 151.1, 150.4, 147.4, 146.7, 124.4, 62.8, 62.1, 49.6, 47.5, 41.9, 29.7, 27.7. ESI-HRMS: $\text{C}_{39}\text{H}_{46}\text{F}_{24}\text{N}_{10}\text{O}_4\text{P}_4$ calcd for m/z = 1153.2623 [$M - \text{PF}_6$]⁺, found m/z = 1153.2644; calcd for m/z = 504.1488 [$M - 2\text{PF}_6$]²⁺, found m/z = 504.1488.

5•4Cl: **5•4PF₆** (100 mg, 0.077 mmol) was dissolved in a minimum amount of MeCN and a saturated aqueous TBACl solution was added dropwise to the resulting solution to afford a precipitate which was filtered and washed with water to give **5•4Cl** (59 mg, 90%) as a beige powder. ^1H NMR (500 MHz, CD_3OD , 298 K): δ = 9.23 (t, J = 7 Hz, 8H), 8.68 (d, J = 6 Hz, 8H), 7.99 (s, 2H), 5.12 (t, J = 6 Hz, 4H), 4.55 (s, 6H), 4.47 (t, J = 6 Hz, 4H), 4.03 (t, J = 6 Hz, 4H), 3.54 (t, J = 6 Hz, 4H), 3.44 (s, 2H), 2.21 (m, 4H). ^{13}C NMR (125 MHz, CD_3OD , 298 K): δ = 168.3, 151.5, 150.8, 148.0, 147.3, 143.2, 128.2, 127.9, 125.4, 63.1, 62.2, 49.8, 49.2, 48.0, 41.9, 30.0, 28.1. ESI-HRMS: $\text{C}_{39}\text{H}_{46}\text{Cl}_4\text{N}_{10}\text{O}_4$ calcd for m/z = 823.2764 [$M - \text{Cl}$]⁺, found m/z = 823.2752.

S3. ^1H and ^{13}C NMR spectroscopy

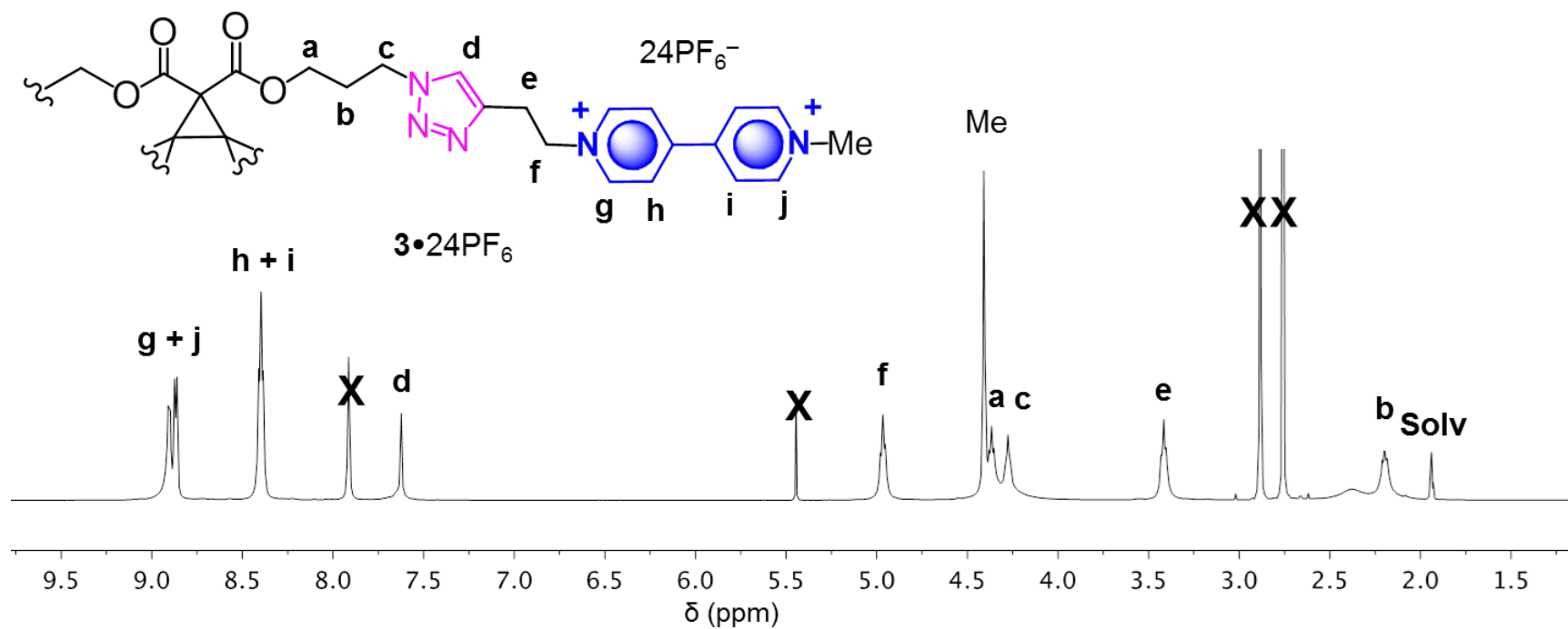


Figure S1. ^1H NMR (500 MHz) spectrum of $3 \cdot 24\text{PF}_6$ in CD_3CN at 298 K

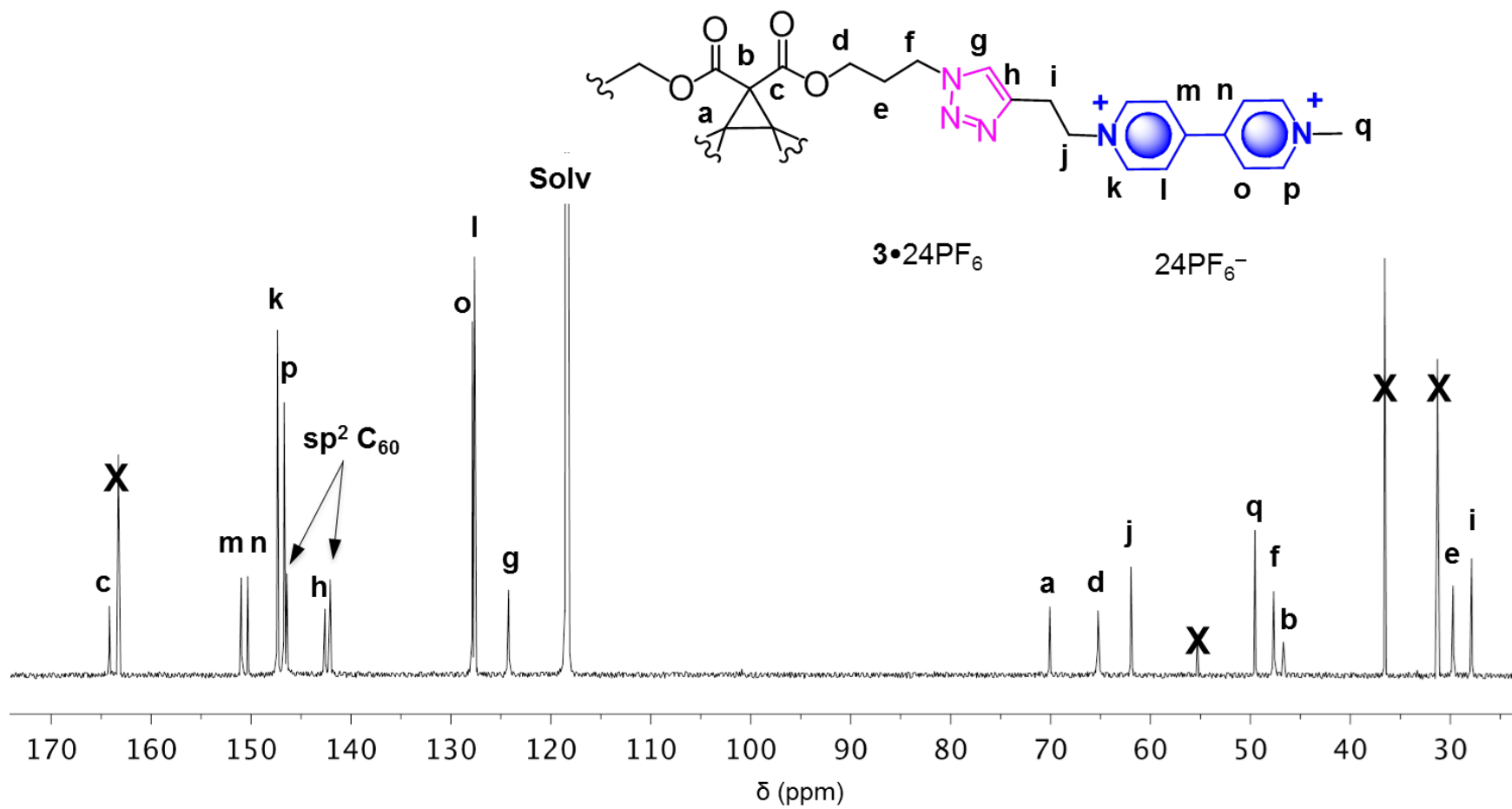


Figure S2. ^{13}C NMR (125 MHz) spectrum of $3 \cdot 24\text{PF}_6$ in CD_3CN at 298 K

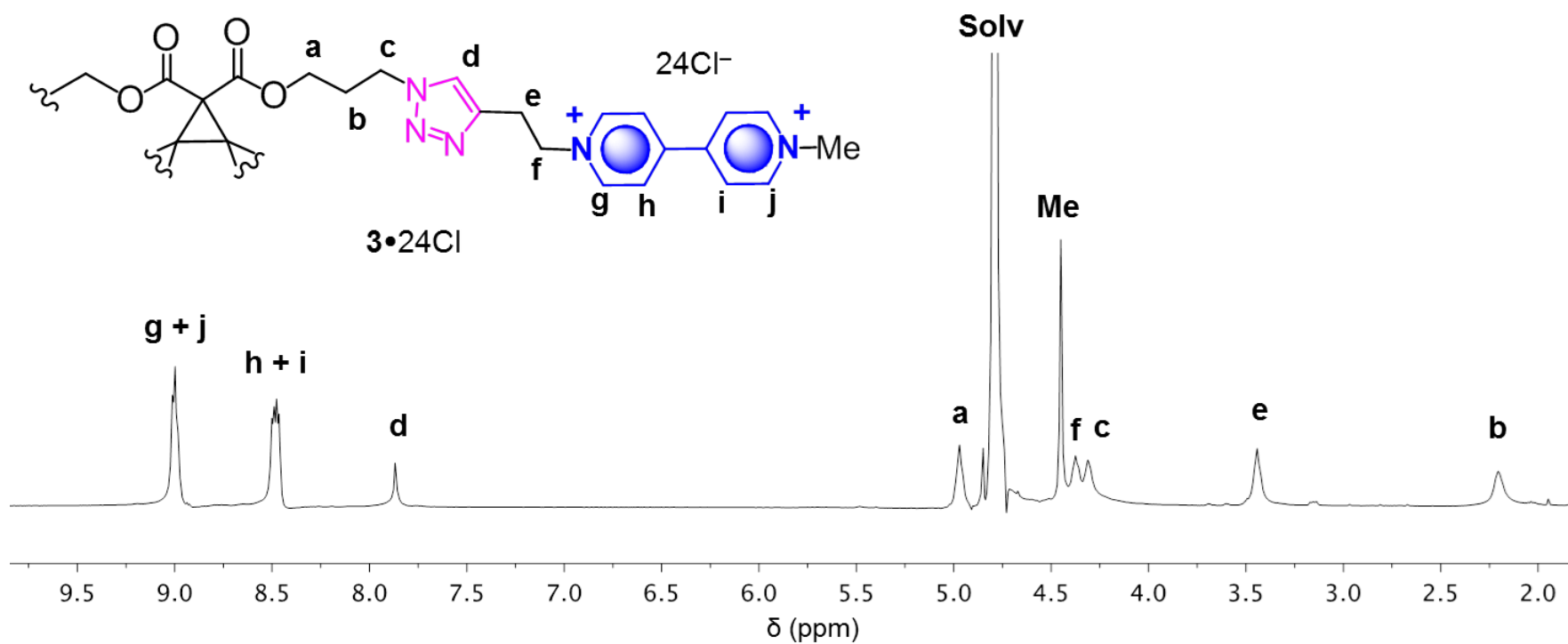


Figure S3. ¹H NMR (500 MHz) spectrum of **3•24Cl** in D₂O at 298 K

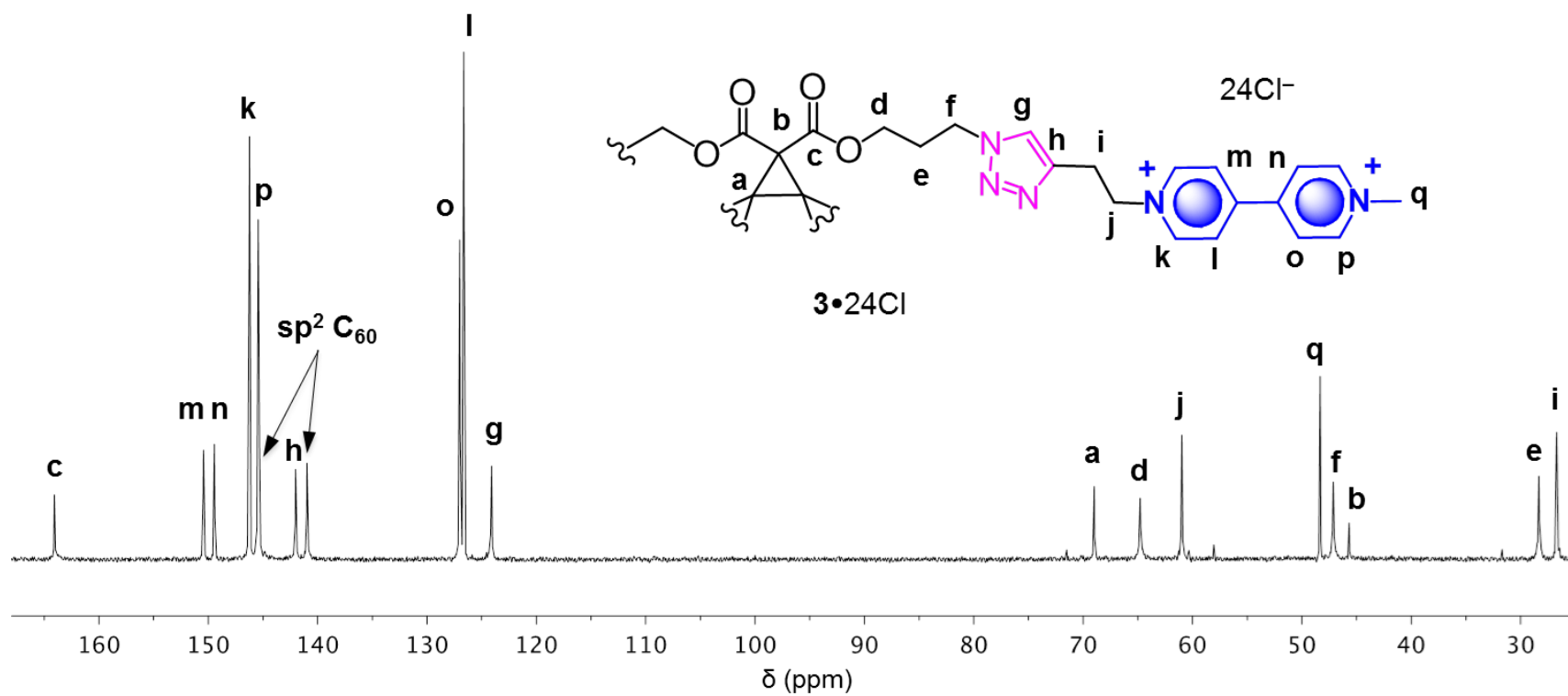


Figure S4. ^{13}C NMR (125 MHz) spectrum of $3 \cdot 24\text{Cl}$ in D_2O at 298 K

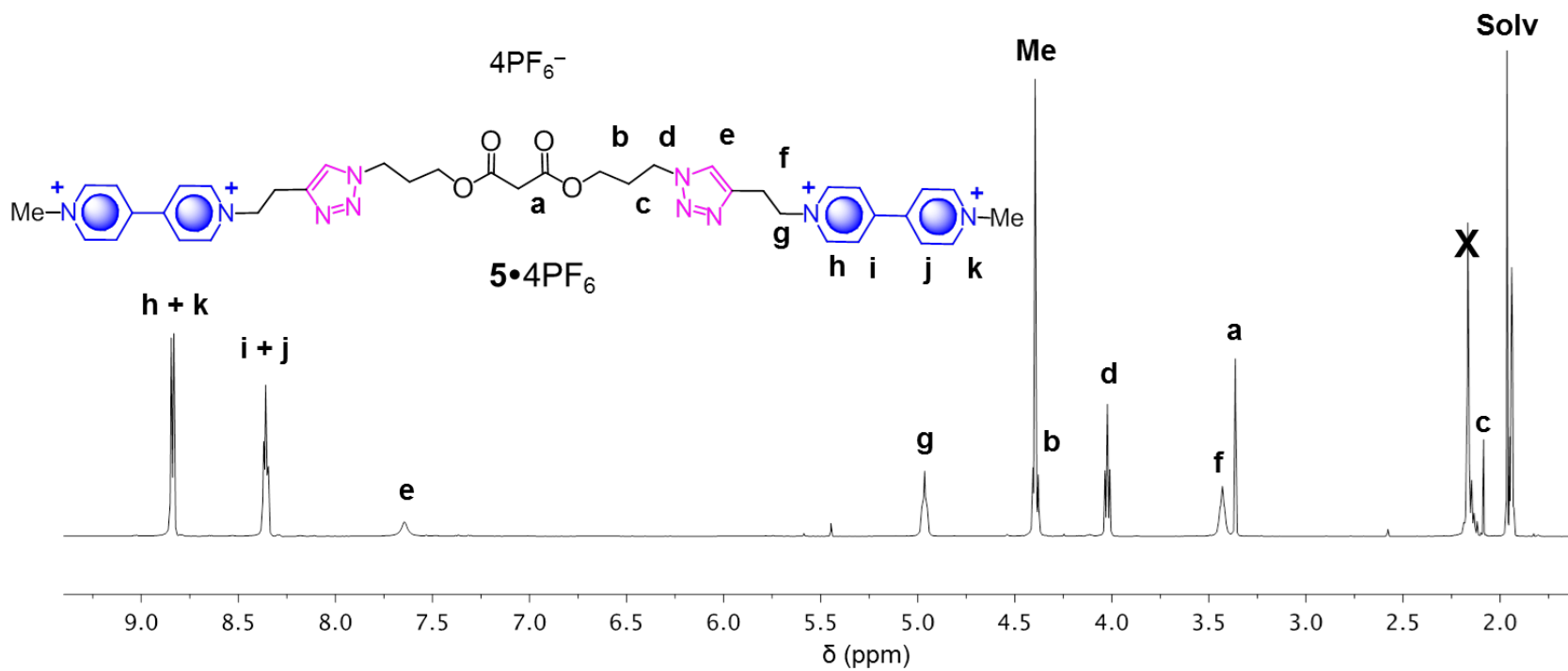


Figure S5. 1H NMR (500 MHz) spectrum of $5 \cdot 4PF_6^-$ in CD_3CN at 298 K

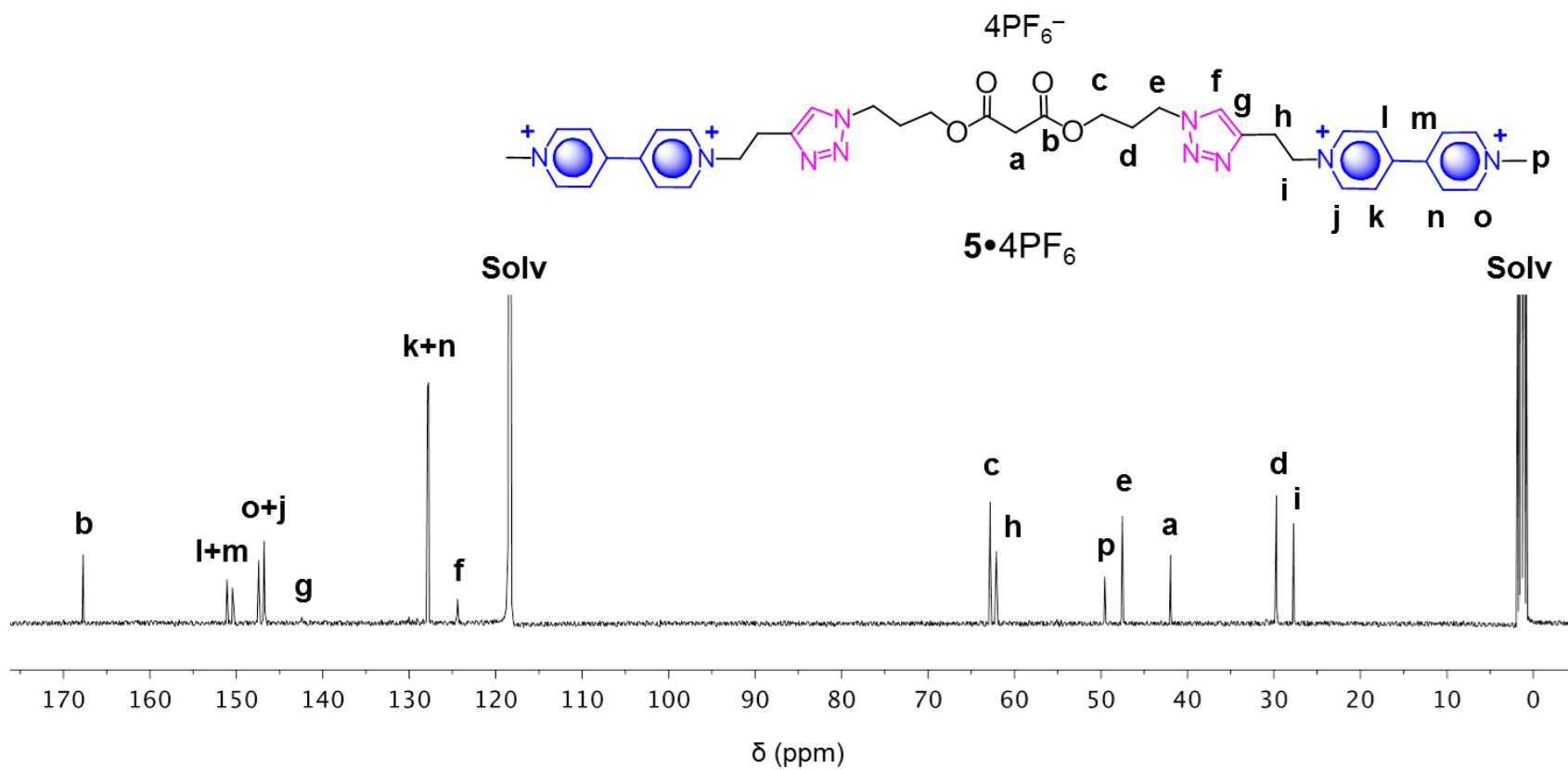


Figure S6. ^{13}C NMR (125 MHz) spectrum of $5 \cdot 4PF_6^-$ in CD_3CN at 298 K

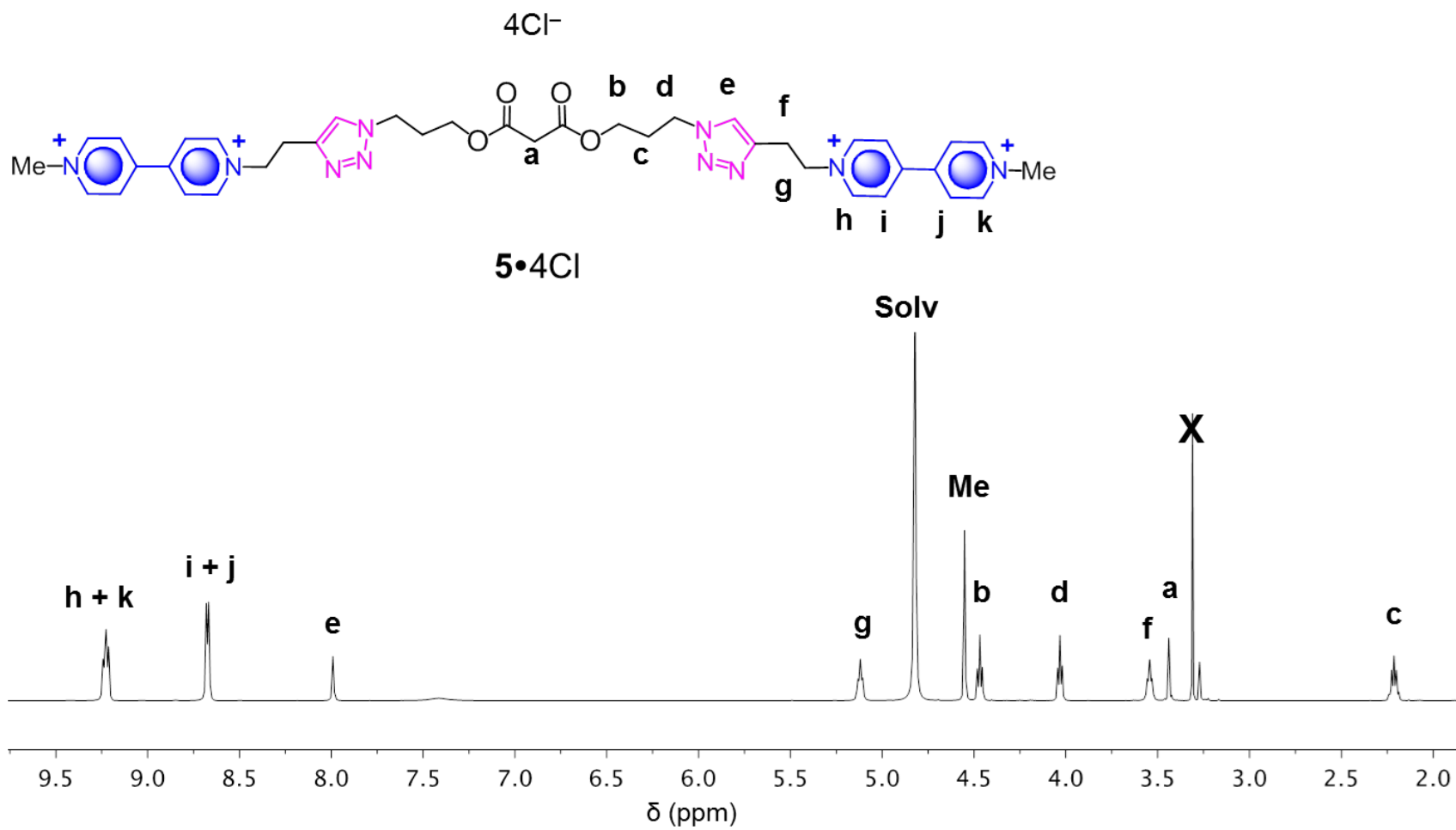


Figure S7. ^1H NMR (500 MHz) spectrum of **5•4Cl** in MeOD at 298 K

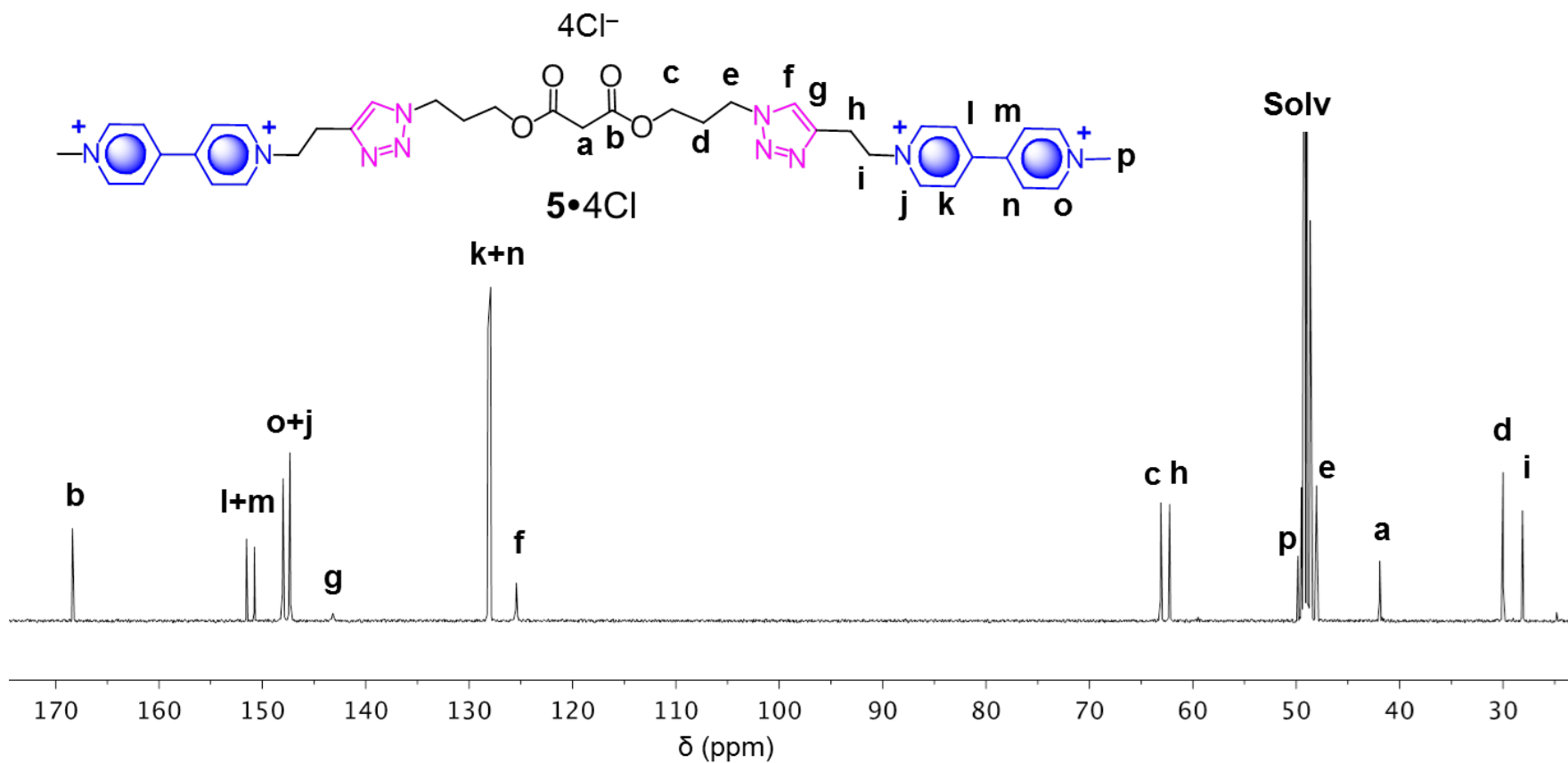


Figure S8. ^{13}C NMR (125 MHz) spectrum of $5 \cdot 4Cl$ in MeOD at 298 K

S4. Mass spectrometry

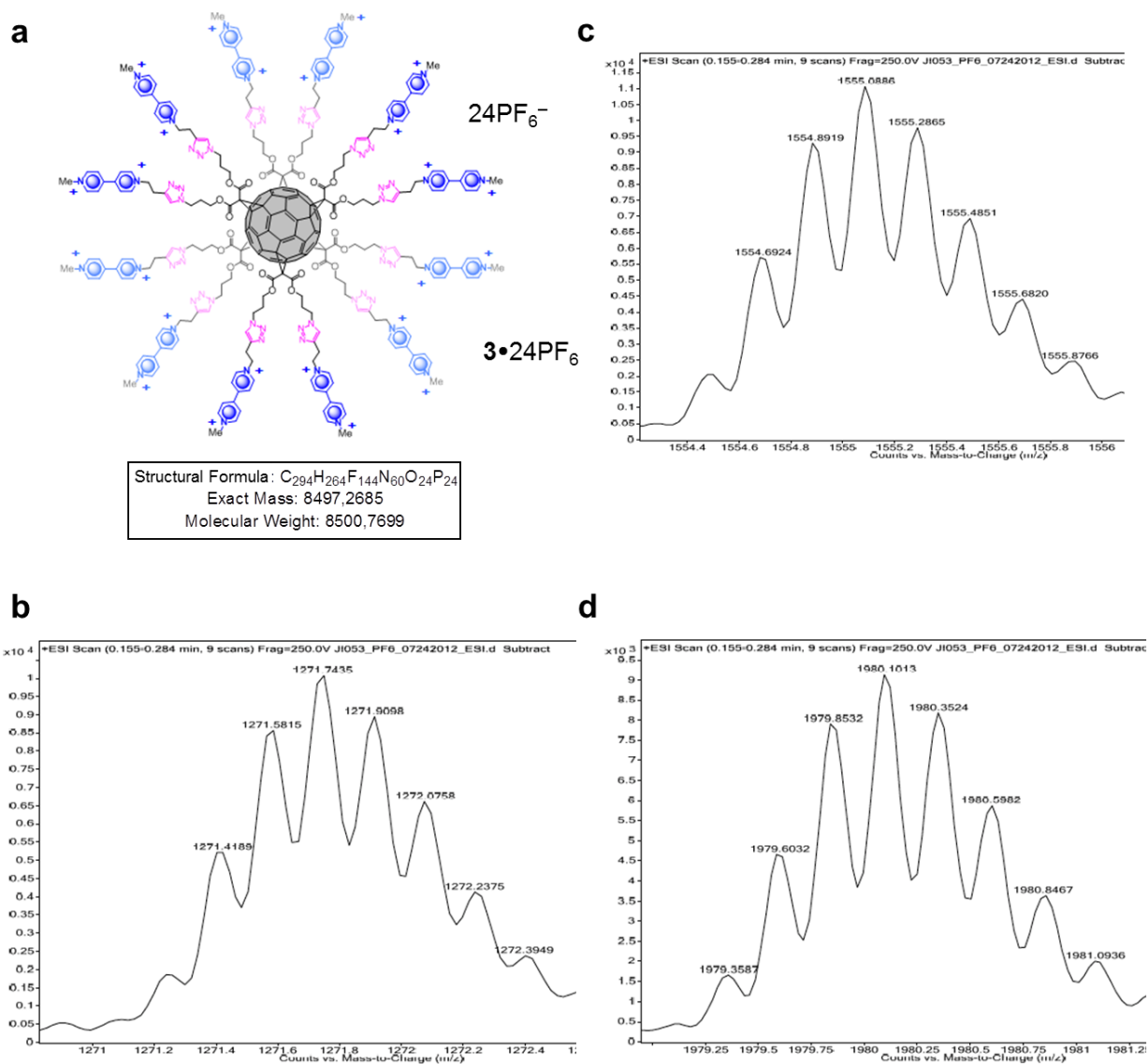


Figure S9. HRMS (ESI) of **3•24PF₆**. a) Structure formula of **3•24PF₆**; PF₆⁻ counterions losses associated with each charge state: b) $[M - 6PF_6]^{6+}$; c) $[M - 5PF_6]^{5+}$ and d) $[M - 4PF_6]^{4+}$

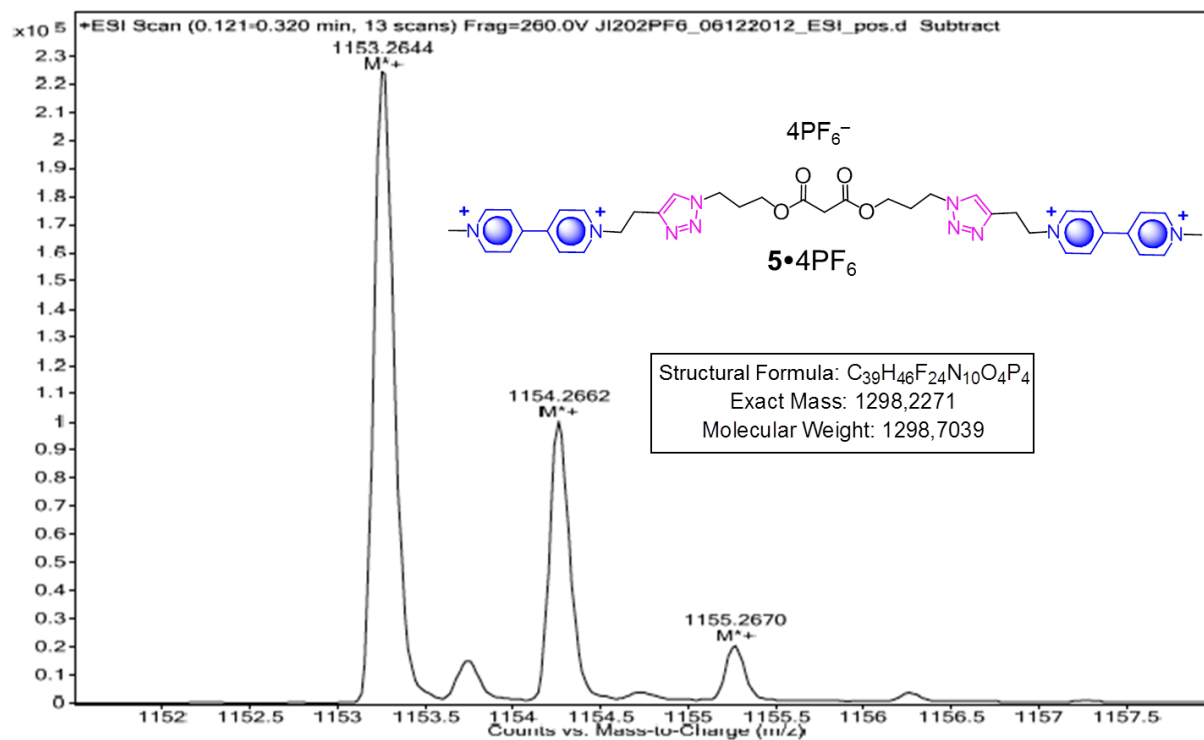


Figure S10. HRMS (ESI) of **5•4PF₆**

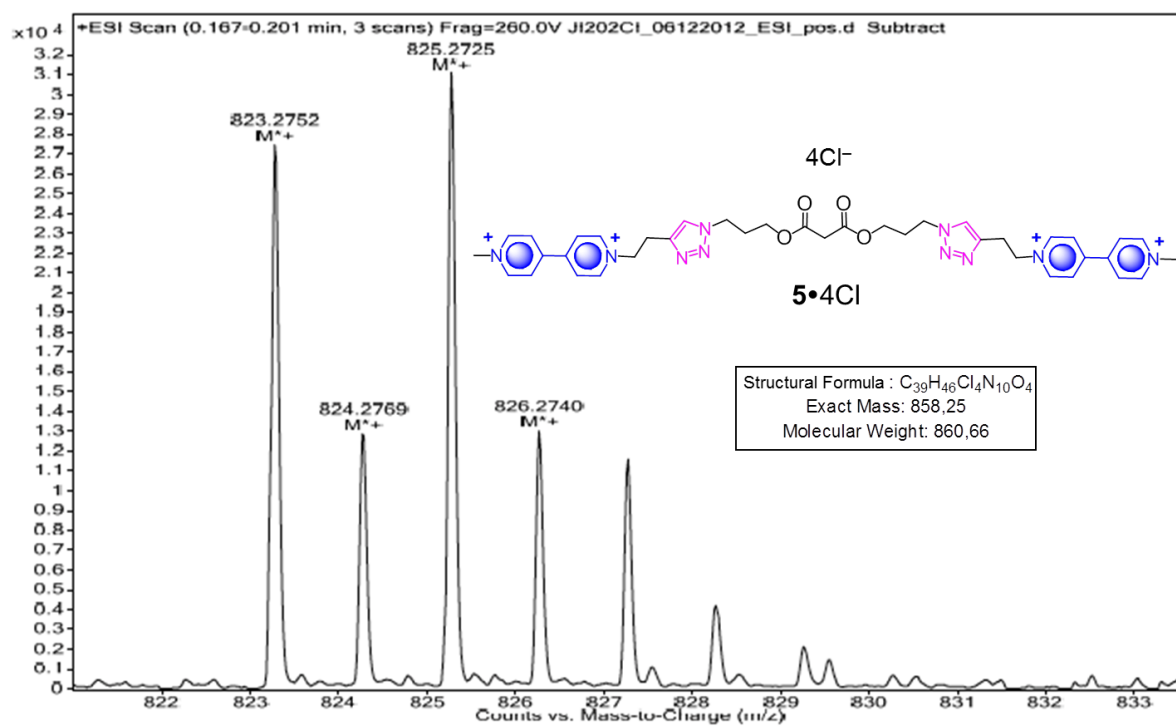


Figure S11. HRMS (ESI) of **5•4Cl**

S5. Electrochemical experiments

Differential pulse voltammetry (DPV) and cyclic voltammetry (CV) measurements

The electrochemical behavior of a solution of 3^{2+} in DMF has been examined by differential pulse voltammetry (DPV). The voltammogram shows the two reduction processes, typical of viologen units. In addition to the observation of the two successive reductions, a cathodic process is identified around -1.38 V versus Ag/AgCl, and has been attributed to the reduction of hexasubstituted C_{60} unit.

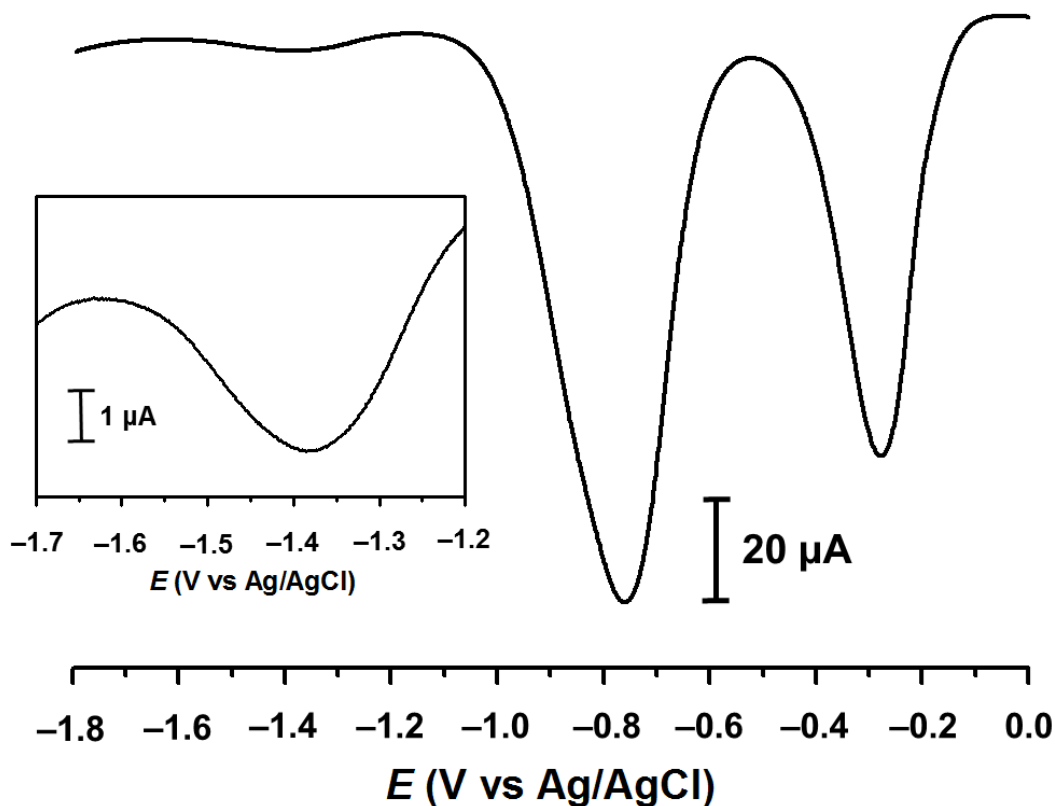


Figure S12. DPV experiments of 3^{2+} recorded in argon-purged DMF solution at a 0.3 mM concentration with TBAPF₆ (0.1 M) as the supporting electrolyte at 298 K.

The electrochemical properties of MV^{2+} , 5^{4+} and 3^{24+} have been investigated in MeCN, using PF_6^- counterions, and in aqueous solution, with Cl^- counterions. Cyclic voltammogram of a MeCN solution of 3^{24+} shows (Figure S13a) that the reducible viologen units around the all-carbon sphere are equivalent and the first reduction ($E_{1/2} = -0.391$ V versus Ag/AgCl) is reversible with Nerstian behavior. In aqueous solution, the first viologen center reduction which is observed at $E_{1/2} = -0.477$ V and -0.546 V for 3^{24+} and 5^{4+} , respectively, occur at significantly less negative potential values, $E_{1/2} = -0.646$ V, than MV^{2+} . The observed shift in the redox potential can be explained by a stronger intramolecular dimerization of two radicals, producing a π -dimer, in aqueous solution.

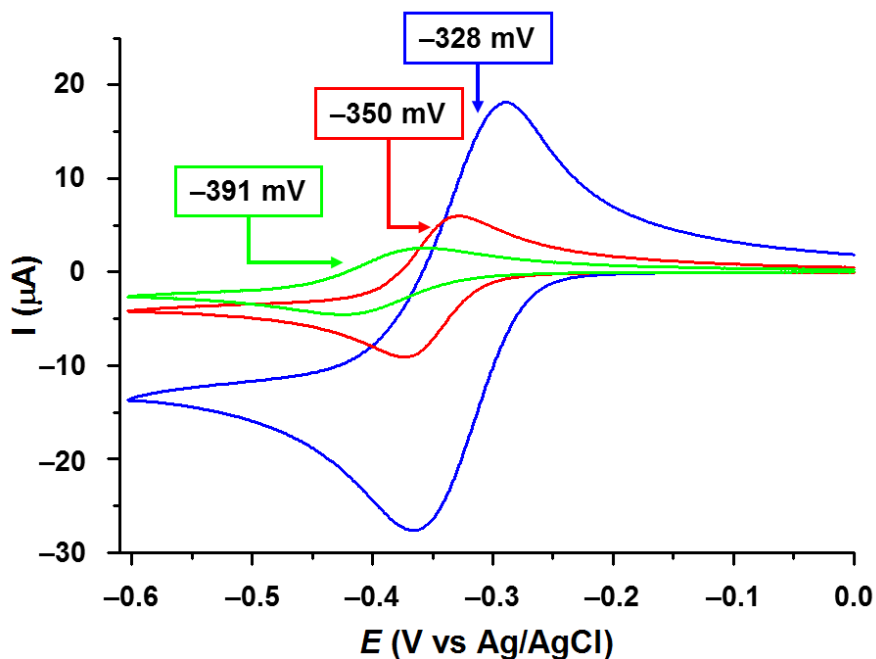


Figure S13. Cyclic voltammograms of MV^{2+} (green line), 5^{4+} (red line) and 3^{24+} (blue line) recorded in MeCN in the presence of 0.1 M $TBAPF_6$. Concentration of all samples were 0.3 mM. All data were recorded at 298 K at a stationary platinum working electrode (E vs Ag/AgCl, $v = 0.050$ V \cdot s $^{-1}$).

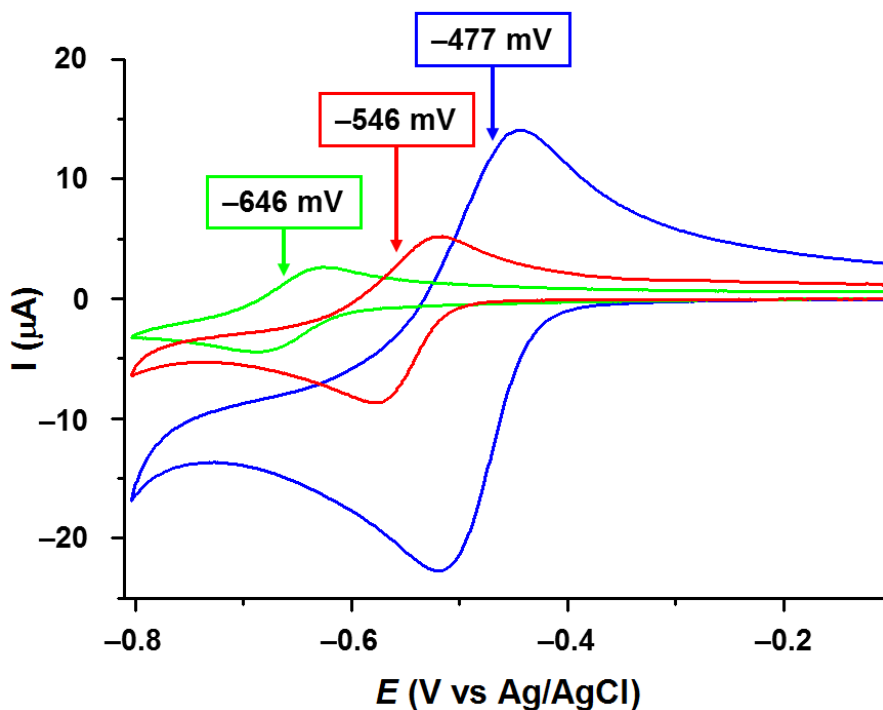


Figure S14. Cyclic voltammograms of MV^{2+} (green line), 5^{4+} (red line) and 3^{24+} (blue line) recorded in 0.1 M phosphate buffer 0.1M (pH 7.0). Concentration of all samples were 0.3 mM. All data were recorded at 298 K at a stationary platinum working electrode (E vs Ag/AgCl, $\nu = 0.050 \text{ V}\cdot\text{s}^{-1}$).

S6. UV/Vis spectroscopy

Spectroelectrochemical experiments 3^{24+} in MeCN were performed in order to obtain the adsorption spectra of the reduced viologen. The electrochemical reduction performed (Figure S15) at -0.30 V led to an increase in the intensity of the signals and growth of a new band at 860 nm which is attributed to the formation of the viologen radical dimers.

Figures S16 and S17 show the UV/Vis absorption spectra of 3^{24+} and after reduction with zinc dust, its radical form $\text{3}^{12(+)}$ in MeCN and H_2O .

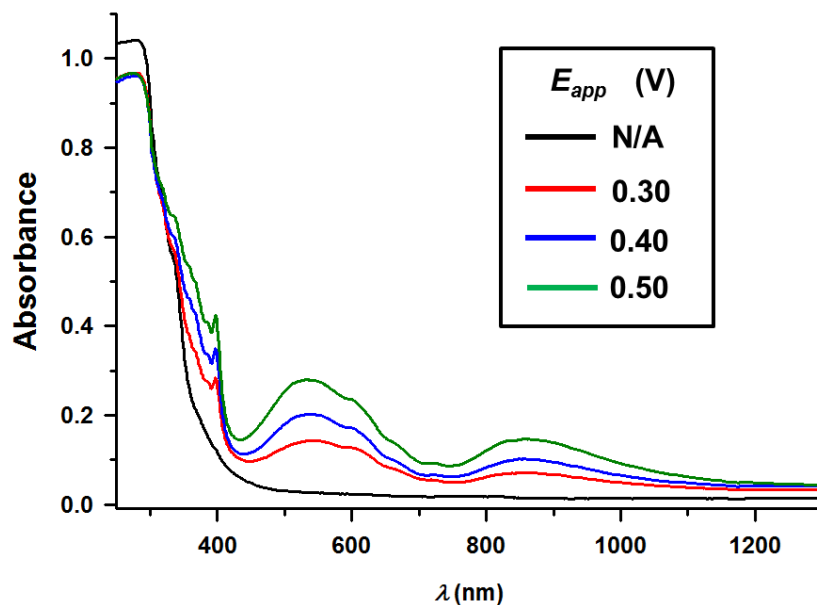


Figure S15. Spectroelectrochemical study of 3^{24+} ($c = 0.3$ mM in MeCN with 0.1 M of TBAPF₆). Before reduction (black trace), and after reduction at -0.30 V (red trace), -0.40 V (blue trace), and -0.50 V (green trace).

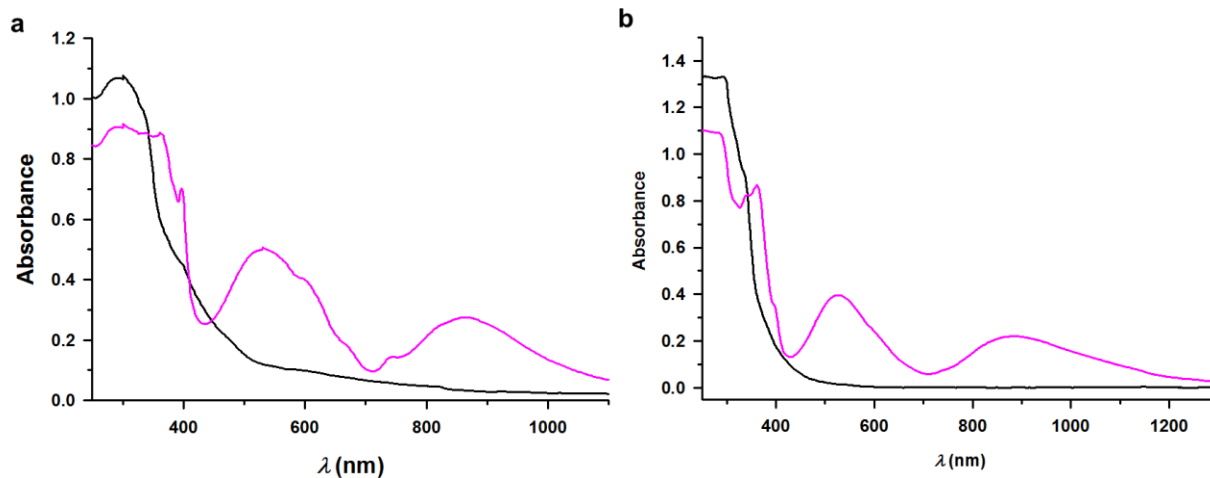


Figure S15. UV/Vis absorption spectra of 3^{24+} (black line) and under its reduced form (purple line) in (a) MeCN and (b) H₂O.

S7. EPR spectroscopy

EPR spectra were recorded for a solution of $3 \cdot 24\text{PF}_6$ and $5 \cdot 4\text{PF}_6$ in MeCN reduced with zinc dust for 30 min, before the EPR measurements.

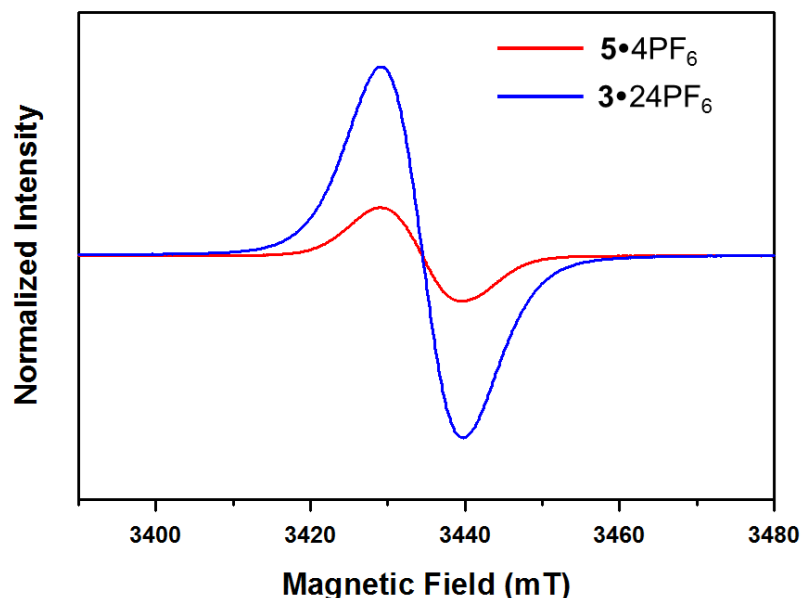


Figure S16. EPR spectra recorded at 298 K from MeCN solutions of 3^{24+} (blue trace) and 5^{4+} (red trace) after reduction.

S8. Computational chemistry

Force field parametrization

As explained in the text the MM3 force field was used to perform all the molecular dynamics simulations. Most of the MM3 parameters required to simulate the dynamics of the 5^{4+} and 3^{24+} molecules are preset in the MM3-2000 parameter set, especially the parameters of the N^+ pyridinium ions. The additional parameters for the PF_6^- ions were taken from the literature.^{S3} Most of these parameters, required to the MM3 force field to perform the calculations, were replaced by the value of analogous systems already included in the force field. For example the out-of-plane bending of $\text{C}(\text{sp}^3)\text{-N}^+$ were replaced by the value of the H-N^+ pair. These

substitutions are of no consequence on the simulation, as reported in previous publications^{S4}.

However the MM3 parameters relative to the carbon atom linking each malonate to the C₆₀ were treated more carefully. In particular the bending and torsional parameters were fitted to first principle calculations. First, the total energy of a minimal complex was computed for different values of the bending and torsional angle. These simulations were performed at the DFT level using 6-31G basis set and the B3LYP functional implemented in the QChem package. The results of this fit are represented in Fig. S17.

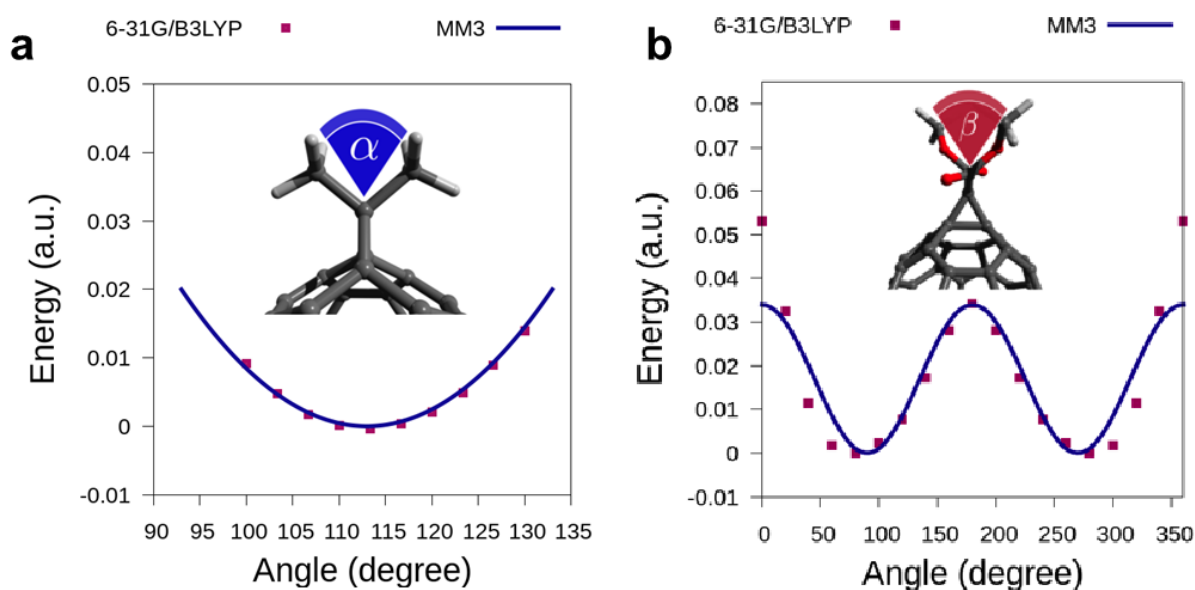


Figure S17. DFT based (6-31G/B3LYP) MM3 parametrization of the bending and torsional parameters of the anchoring carbon atom.

The energy obtained varying the bending angle can be fitted with the usual elastic energy term:

$$E_{\alpha} = \frac{1}{2}k_{\alpha}(\alpha - \alpha_0)^2$$

Fitting the results of the DFT calculation with this analytical expression leads to a bending energy of $k_{\alpha} = 0.34$ kcal/mol/rad² and a relaxed bending angle of $\alpha_0 = 113^{\circ}$. The value of the

equilibrium angle is close from the one obtained with C(sp³)-C(sp²)-C(sp³), i.e. (117°) but with a reduced bending energy ($k_{\alpha} = 0.57$ kcal/mol/rad²).^{S5} To compute the torsional parameters, the bending angle was set to its equilibrium energy and the proper dihedral angle was then varied. The energy obtained via the DFT calculations for these different values of the torsion angle can be approximated by the equation^{S5}:

$$E_{\beta} = V_1(1 + \cos(\beta)) + V_2(1 - \cos(2\beta)) + V_3(1 + \cos(3\beta))$$

Fitting the DFT calculations with this curve leads to $V_2 = 10.66$ kcal/mol and the other parameters set to 0 which is a typical values for energy rotation barrier.^{S5}

Minimum energy configuration

Simulated Annealing simulations were employed to determine the minimum energy configuration of the **5**⁴⁺ and **3**²⁴⁺ molecules, in explicit MeCN solvent (50x50x50 Å³ box size, solvent density 0.3 g/cm³). During these simulations the system was first thermalized for 100 ps at 300 K and subsequently cooled down to 0 K in 100 ps using a linear temperature ramp. The simulations were done in the NVT ensemble with a Nose-Hoover chain thermostat with a 1 fs integration time using the Tinker package. These simulations converge to the minimum energy configurations. As explained in the text, steric hindrance prevents the malonates to unfold around the **3**²⁴⁺ complex as observed for isolated malonates.

Molecular dynamics

From the minimum energy conformation isolated by simulated annealing, molecular dynamics were employed to study the temporal behavior of the **5**⁴⁺ and **3**²⁴⁺ molecules. These simulations were performed at 300 K for 3000 ps with a 1fs integration time. The conditions used during the

SA (50x50x50 Å³ box size, solvent density 0.3 g/cm³ 1fs integration time) were used during these MD simulations. The trajectory of the terminal N⁺ ion of each viologen units is represented in Fig. S19.

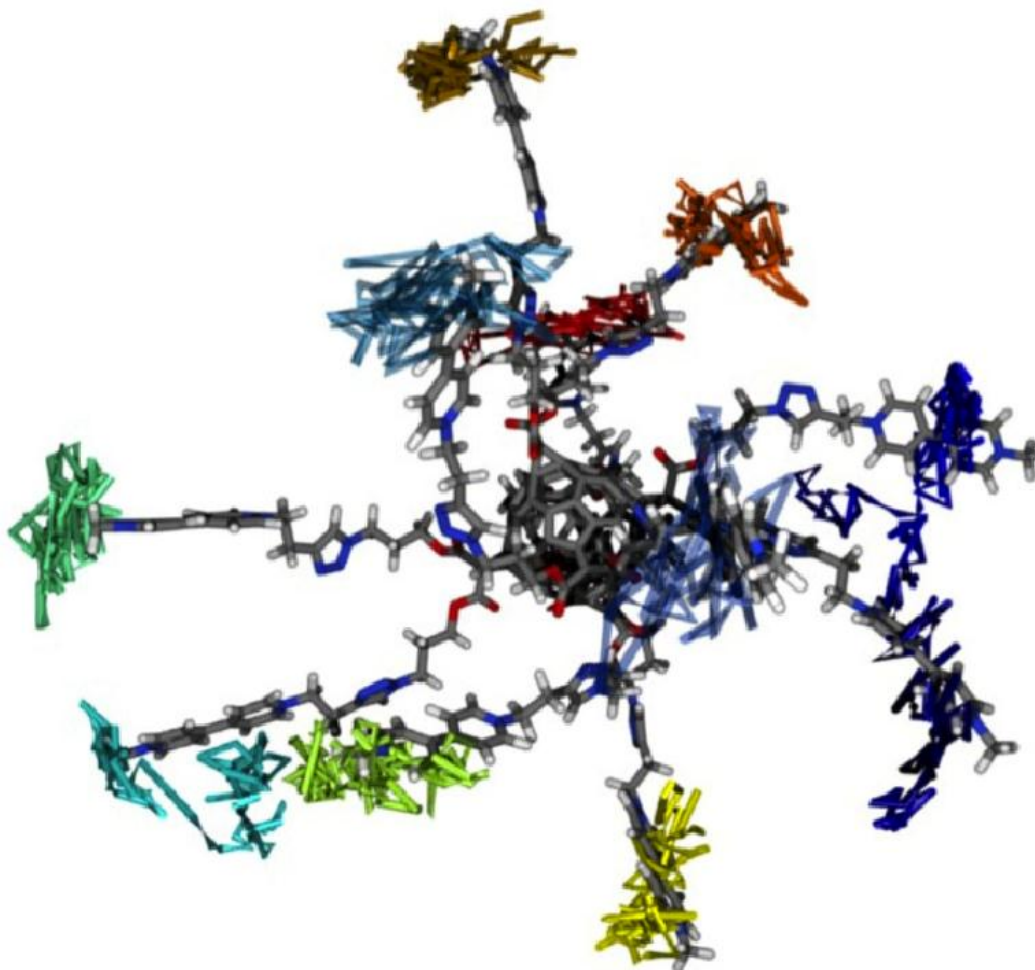


Figure S19. Trajectory of the terminal N⁺ ion during the MD simulations.

The flexibility of the malonates chain should allow the viologen units to explore a very large phase space. However this flexibility is reduced by the presence of the positive charges that forces the viologen units to repel each other. The MD simulations also reveal two stable conformations for the malonate units that can adopt the open or closed geometries represented in

Fig. S20. In the closed geometry, *pi*-merization of the partially aromatic triazole rings compensates for the electrostatic repulsions induced by the proximity of the positive charges.

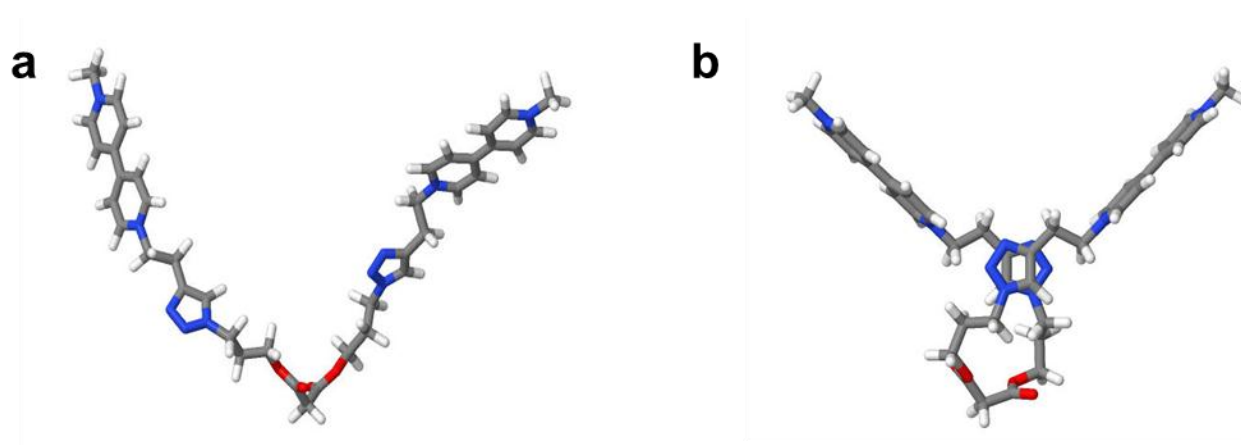


Figure S20. Open and closed configurations transiently adopted by malonates during the MD simulations of the 5^{4+} molecule at room temperature. In the closed form, partial *pi*-merization of the partially aromatic triazole rings compensates for the increased electrostatic repulsion induced by the proximity of the charges.

S9. Supplementary references

- S1 J. Iehl, R. Pereira de Freitas, B. Delavaux-Nicot and J.-F. Nierengarten, *Chem. Commun.*, 2008, **44**, 2450–2452.
- S2 H.-B. Bu, G. Götz, E. Reinold, A. Vogt, S. Schmid, J. L. Segura, R. Blanco, R. Gómez and P. Bäuerle, *Tetrahedron*, 2011, **67**, 1114–1125.
- S3 O. Borodin, G. D. Smith, R. L. Jaffe, *J. Comput. Chem.* 2001, **22**, 641–654.
- S4 I. Franco, M. A. Ratner, G. Schatz, *J. Phys. Chem. B*, 2011, **115**, 2477–2484.
- S5 J.C. Tai, L. Yang, N. L. Allinger, *J. Am. Chem. Soc.* 1993, **115**, 11906–1190.

